Received: 5 March 2024 | Accepted: 22 April 2024
DOI: 10.1002/ame2.12433

ORIGINAL ARTICLE

Adipose-derived mesenchymal stem cell-incorporated PLLA porous microspheres for cartilage regeneration

Chang Gao[1] | Wenlong Yuan[1] | Dongcheng Wang[1] | Xin Zhang[1] | Tong Zhang[2] | Zhimin Zhou[1]

[1]Biomedical Barriers Research Center, Institute of Biomedical Engineering, Chinese Academy of Medical Sciences & Peking Union Medical College, Tianjin Key Laboratory of Biomedical Materials, Tianjin, China

[2]Clinical Laboratory, Tianjin Hospital, Tianjin, China

Correspondence
Tong Zhang, Clinical Laboratory, Tianjin Hospital, Tianjin 300211, China.
Email: zttsmkx@163.com

Zhimin Zhou, Biomedical Barriers Research Center, Institute of Biomedical Engineering, Chinese Academy of Medical Sciences & Peking Union Medical College, Tianjin Key Laboratory of Biomedical Materials, Tianjin 300192, China.
Email: zhouzm@bme.cams.cn; zhouzhiminf@126.com

Funding information
CAMS Innovation Fund for Medical Sciences, Grant/Award Number: 2021-I2M-1-052; Tianjin Hospital Fund for Science and Technology, Grant/Award Number: Tjyy2109; Tianjin Natural Science Foundation for Jingjinji Collaboration, Grant/Award Number: 23JCZXJC00240; Capital's Funds for Health Improvement and Research, Grant/Award Number: CFH: 2022-2-5072

Abstract

Background: In facial plastic surgery, patients with nasal deformity are often treated by rib cartilage transplantation. In recent years, cartilage tissue engineering has developed as an alternative to complex surgery for patients with minor nasal defects via injection of nasal filler material. In this study, we prepared an injectable nasal filler material containing poly-L-lactic acid (PLLA) porous microspheres (PMs), hyaluronic acid (HA) and adipose-derived mesenchymal stem cells (ADMSCs).

Methods: We seeded ADMSCs into as-prepared PLLA PMs using our newly invented centrifugation perfusion technique. Then, HA was mixed with ADMSC-incorporated PLLA PMs to form a hydrophilic and injectable cell delivery system (ADMSC-incorporated PMH).

Results: We evaluated the biocompatibility of PMH in vitro and in vivo. PMH has good injectability and provides a favorable environment for the proliferation and chondrogenic differentiation of ADMSCs. In vivo experiments, we observed that PMH has good biocompatibility and cartilage regeneration ability.

Conclusion: In this study, a injectable cell delivery system was successfully constructed. We believe that PMH has potential application in cartilage tissue engineering, especially in nasal cartilage regeneration.

KEYWORDS
centrifugation perfusion, chondrogenesis, hyaluronic acid, nasal fillers, PLLA porous microspheres

1 | INTRODUCTION

Trauma and congenital malformations can cause craniofacial cartilage defects, such as nasal deformities leading to an unsightly nose. Carved rib cartilage transplantation is a commonly used technique in facial plastic surgery, particularly for treating nasal deformities after cleft lip surgery.[1] However, donor site morbidity, chest wall contour deformity, pneumothorax, and the complicated operation are the main limitations of this classic reconstruction technique.[2] In particular, in the case of minor nasal defects, clinicians have proposed nonsurgical nasal repair and a reduction in the amount of rib cartilage utilized, stimulating the development of injectable fillers or microscaffolds for cartilage cell transplantation.[3] Compared to various gel or particulate fillers for simple volume increases, microcarriers for cell delivery provide a promising option for patients seeking noninvasive techniques for tissue regeneration.[4–8]

The best scaffolds exhibit good biocompatibility and biodegradability, and sufficient porosity and mechanical strength to facilitate cell adhesion, nutrient diffusion, and waste removal for optimal tissue regeneration.[9,10] Among the many tissue repair materials available, polymeric bulk scaffolds stand out for their ability to create a suitable environment for accelerated tissue healing. Alternatively, organic or inorganic microspheres have attracted increased attention for use in tissue repair due to their ability to promote efficient cell proliferation and easy manipulation.[6,7,11–13] These as-prepared microspheres are generally employed to repair different tissues, including periodontal tissue, adipose tissue, cartilage and pancreatic islets. They can be directly used not only as cell delivery carriers, but also to create composite scaffolds with enhanced mechanical properties.[6,9,14–18] Notably, compared with their nonporous counterparts, porous microspheres (PMs) can provide larger voids for cell seeding, exhibiting a greater cartilage regeneration ability.[5,19] In addition, modification with hydrophilic biomacromolecules or signal molecule incorporation is a routine strategy to improve cell attachment and proliferation in the hydrophobic poly(lactic-co-glycolic acid) (PLGA) or poly-L-lactic acid (PLLA) scaffolds.[20,21] Hyaluronic acid (HA) is a natural component of the extracellular matrix and a typical hydrophilic material that can enhance the hydrophilicity and water-binding ability of microspheres.[9] HA is often used to prepare composite scaffolds for tissue regeneration or to simply act as a formulation agent of particulate fillers for convenient injection.[5,22,23]

In addition to the porous structure and hydrophilic modification of various microcarriers, cell seeding method is also a key parameter for constructing artificial organs or cell delivery systems for more efficient tissue regeneration.[6,15,19] Our group recently invented a cell centrifugation perfusion technique that demonstrated superior cell-loading efficacy compared to traditional cell incubation techniques during artificial pancreatic islet construction based on PLGA PMs.[15] Therefore, it is feasible to develop an injectable stem cell delivery system that combines a porous structure, hydrophilic modifications and highly efficient cell seeding technique instead of traditional bulk scaffolds for craniofacial cartilage regeneration.[17,24]

Adipose-derived mesenchymal stem cells (ADMSCs), which are easily obtained from adipose tissue, show good potential for tissue regeneration due to their ability to proliferate and differentiate in multiple directions.[25] Compared to MSCs from bone marrow, ADMSCs show fewer signs of aging.[26] In addition, for stem cell therapy, ADMSCs offer several distinct advantages, including longer-term storage, greater stability, and more convenient availability via liposuction. However, treatment involving the injection of stem cells alone has unsolved problems, such as a low cell survival rate and short cell retention time, which may result in unsatisfactory therapeutic outcomes.[27] Although polymeric PMs can be used as carriers for ADMSCs to increase cell adhesion, proliferation, and differentiation, long-term in vitro culture can affect the functions and fate of the cells.[28] Immediate injection has been proposed to mitigate these side effects and enhance treatment efficacy.[5] Therefore, construction of an ADMSC delivery system suitable for immediate injection based on our previous use of polymeric PMs for tissue engineering and centrifugation perfusion for cell seeding is needed.[6,9,15,24]

Herein, we seeded ADMSCs into as-prepared PLLA PMs using our invented centrifugation perfusion technique.[6,15] Then, HA was mixed with ADMSC-incorporated PLLA PMs to form a hydrophilic and injectable cell delivery system (ADMSC-incorporated PMH). The differentiation, viability, and proliferation of the cells were evaluated in vitro. Finally, ADMSC-incorporated PMH was injected subcutaneously into nude mice to investigate cartilage regeneration in the presence or absence of cartilage cells.

2 | METHODS

2.1 | Materials

PLLA (M_w: 150,000) was purchased from Shandong Academy of Pharmaceutical Sciences. Tianjin Fengchuan Chemical Reagent Technology provided dichloromethane (CH_2CL_2) and sodium hydroxide (NaOH). Shanghai Aladdin Biochemical Technology supplied ammonium bicarbonate (NH_4HCO_3). Sodium hyaluronate $(C_{14}H_{20}NO_{11}Na)_n$ was purchased from Bloomage Biotechnology Corporation Limited. All other chemical reagents were of analytical grade and obtained from commercial sources.

2.2 | Preparation of PMH

PLLA PMs were prepared by the double emulsion method as described in our previous publication.[17] In addition, 100 mg of HA powder was weighed and fully dissolved in 10 mL of sodium chloride solution overnight, resulting in a 1% HA solution. The desired amount of PLLA PMs and 10 mL of HA were placed in a vial, and an injection syringe was used to repeatedly draw in and expel the resulting solution, ensuring that the PLLA PMs were evenly dispersed in the HA solution to form PMH.

2.3 | Physical characteristics

2.3.1 | Morphology

The PLLA PMs, HA, and PMH were lyophilized, then sliced and fixed on a copper plate containing conductive adhesive, and then coated with a layer of metal. The morphologies of the PLLA PMs, HA, and PMH were observed by scanning electron microscopy (SEM, Carl Zeiss Merlin Compact, Baden-Wurttemberg, Germany). ImageJ was used to analyze the obtained SEM images, and the average particle sizes and pore sizes ($n = 50$) of the PLLA PMs were measured.

2.3.2 | Rheological properties

The rheological properties of HA and PMH were measured by a rheometer (Modular Compact Rheometer, Anton Paar, Austria). The shear viscosity (η) and shear stress (τ) of the HA solution and PMH in the range of 0.1–100 S^{-1} shear rate (γ) were measured at 37°C to determine the relationships among η, τ and γ.

2.3.3 | Injectability

The injectability of PMH was explored using four samples of PMH and four samples of pure (control) PLLA PMs suspended in ultrapure water. Control PLLA PMs and PMH without injection were used as the control group. The remaining six groups were passed through syringes with 16G (Ø 1.65 mm), 22G (Ø 0.71 mm), or 25G (Ø 0.51 mm) needles. To more clearly observe the morphological changes to PLLA PMs in the PMH, we washed the four PMH samples three times with deionized water, and collected the PLLA PMs. Changes in the volume and morphology of the control PLLA and PMH groups were observed.

2.4 | Primary culture and identification of ADMSCs

Female New Zealand white rabbits weighing 3 kg were used in this study. All the procedures in this study were performed with permission from the Animal Ethical and Welfare Committee of the Experimental Animal Center of the Institution of Radiation Medicine, Chinese Academy of Medical Sciences. Adipose tissue extracted from the inguinal region of the rabbits was digested in a solution containing 1 mg/mL type I collagenase (Gibco, Carlsbad, CA, USA) at 37°C for 1 h and then filtered through a 100 μm filter to obtain a single-cell suspension. The single-cell suspensions were subsequently seeded in complete DMEM-F12 (Gibco) supplemented with 20% (v/v%) fetal bovine serum (Gibco), 100 μg/mL penicillin, and 100 μg/mL streptomycin (Gibco). The cells were incubated at 37°C with 5% CO_2 in a humidified incubator. Flow cytometry was used to identify ADMSCs with antibodies against CD29 and CD34. Oil Red O staining, Alizarin Red staining, and Alcian Blue staining were used to assess the multilineage differentiation potential of the ADMSCs.

2.5 | ADMSC proliferation and viability in PMH

A dish of cells showing good growth was taken and used to make a cell suspension. ADMSCs were perfused into PLLA PMs using our own technique of 'centrifugal infusion'.[15] The sample was then mixed with an appropriate amount of HA to produce PMH loaded with ADMSCs. Using the centrifugal infusion method, we prepared PMH loaded with ADMSCs with HA:PLLA PM ratios of 10:1, 10:3, and 10:5. A sample of PLLA PMs loaded with ADMSCs was used as the control sample (containing the same amount of PLLA PMs as in the above 10:3 HA:PLLA PM sample). The above samples were placed in a 6-well plate and cultured normally after the appropriate amount of culture medium was added. DNA was extracted from each sample after 1, 4, and 7 days to verify the proliferation of ADMSCs in PLLA PMs and PMH. DNA was extracted using an Animal Tissue/Cell Genomic DNA Extraction Kit (Solarbio, Beijing, China). Then, 20 μL of DNA was added to a 96-well plate with 180 μL of Hoe Chst 33258 working solution in the dark. Finally, the absorbance was measured by microplate reader at an excitation wavelength of 356 nm and an emission wavelength of 492 nm.

To further explore cell growth inside the PMH, we used live-dead cell staining to directly observe cell activity inside the carrier. Staining was carried out according to the steps described for the calcein-AM/PI Kit (Solarbio, Beijing, China). First, 1 mL of 1× Assay Buffer was added to the confocal dish. Then, 2 μL of calcein-AM (stock solution) was added to the above mixture, and the mixture was incubated in the confocal dish for 25 min at 37°C in the dark. A 4 mL aliquot of PI stock solution was then added to the above confocal dish for 5 min at 37°C in the dark, after which the stained samples were observed using a confocal microscope to distinguish live and dead cells. In this way, the growth of cells in PMH was visually observed, and their activity was determined.

2.6 | Gene expression analysis and TNF-α release

The ADMSC group and the ADMSC-incorporated PMH group were seeded in 6-well plates. After 48 h of culture, we added chondrogenic differentiation induction solution containing the adipose stem cells to the system. After 28 days of induction, chondrogenic ADMSCs were obtained from the ADMSC group and the ADMSC-incorporated PMH group. The mRNAs of the ADMSC group and the ADMSC-incorporated PMH group were extracted, and the obtained mRNA samples were reverse transcribed using an RT–PCR kit (TaKaRa, Beijing, China) to obtain single-stranded cDNA. Real-time fluorescence quantitative PCR was used to detect the expression of cartilage formation markers, including SOX9, ACAN, and COL2A1. GAPDH was used as the endogenous reference gene, and the relative expression was calculated by the $2^{-\Delta\Delta Ct}$ method. A list of forward and reverse primer pairs and their abbreviations is shown in Table 1.

The complete medium was prepared by adding 1% sodium pyruvate, 1% double antibody and 5% FBS to DMEM. RAW264.7 cells were cultured in a 37°C cell incubator. When the cells reached 80% confluence, PLLA PMs and PMH were added separately and incubated with the cells for 24 h, after which the supernatant was collected. The supernatant of RAW264.7 cells without any additions was used for the control group. The tumor necrosis factor-α (TNF-α) concentration in each sample was determined according to the experimental protocol

Gene	F′	R′
GAPDH	CCACTTTGTGAAGCTCATTTCCT	TCGTCCTCCTCTGGTGCTCT
COL2A1	ACGCTCAAGTCCCTCAACAAC	ATCCAGTAGTCACCGCTCTTCC
SOX9	GCTCCGACACCGAGAATACAC	CTTGTCCTCTTCGCTCTCCTTC
ACAN	CTCCAATGACTCCGGGATCTAC	CCTTTCACCACCACCTCCA

TABLE 1 Primer sequences used for real-time PCR.

provided with the Mouse TNF-α ELISA Kit (Invitrogen, Carlsbad, CA, USA). The detection antibody (50 μL/well) was added to a 96-well plate containing the sample supernatant and the capture antibody and incubated at room temperature for 2 h. After washing 4 times, horseradish peroxidase-labeled streptavidin (streptavidin HRP) was added, and the mixture was incubated for 1 h. After another 4 washes, 100 μL of chromogenic agent (TMB) was added to each well, and the mixture was incubated under dark conditions. Subsequently, the stop solution was added, and the concentration of TNF-α in the supernatant of each sample was determined via absorbance at 450 nm.

2.7 | *In vivo* evaluation of chondrogenesis

Animal experiments were carried out to evaluate the in vivo compatibility and cartilage formation potential of ADMSC-incorporated PMH. The animal experiment was approved by the Animal Ethical and Welfare Committee of the Experimental Animal Center of the Institution of Radiation Medicine, Chinese Academy of Medical Sciences. Sixteen 6-week-old female BALB/c nude mice weighing between 17 and 21 g were selected and randomly divided into two groups, namely, the ADMSC/PMH group and the ADMSC+Rabbit ear chondrocytes (REC)/PMH group, based on subcutaneous injection of ADMSC-incorporated PMH with or without RECs. The ADMSCs used during the animal experiment period were induced in vitro for 28 days. RECs were used to establish a chondrogenic environment for the induction of ADMSCs. During the experiment, all the mice were maintained under IVC conditions. Four and eight weeks after injection, the nude mice were sacrificed, and the desired tissues were dissected with scissors and tweezers for further study. Tissues were fixed in 4% paraformaldehyde for 48 h and then dehydrated in 30% sucrose aqueous solution. After the samples were embedded in optimal cutting temperature compound, the sections were cut into 8 μm thick sections using a microtome (Leica, Germany). H&E staining was carried out to evaluate the distribution of chondrocytes. Alcian Blue staining was used to evaluate the deposition of glycosaminoglycan (GAG). Immunohistochemical staining of type II collagen was used to observe the secretion of type II collagen.

2.8 | Statistical analysis

All the statistical calculations were performed with SPSS 21.0 (SPSS, Inc., Chicago, IL, USA) statistical software. The data are presented as the mean ± standard deviation (SD). Student's *t* test or one-way analysis of variance (ANOVA) was performed to determine statistical significance. A p value ≤ 0.05 was considered to indicate statistical significance.

3 | RESULTS

3.1 | Fabrication of PLLA PMs and PMH

Figure 1A,B show that the PLLA PMs had a spherical shape with large and interconnected pores. The diameter of these particles was 100–400 μm, with an average diameter of 258.93 μm (Figure S1A). The pore size was 8.93–63.78 μm, with an average pore size of 24.25 μm (Figure S1B), which provided a 3D microenvironment for cell infiltration and proliferation.[15,29] While mixing PLLA PMs with HA, we observed that the PLLA PMs were uniformly distributed in HA (Figure 1C,D). HA did not change the porous structure of the PLLA PMs but could stabilize the PMs and increase the injectability of PMH because of the fluidic nature of the HA solution.[5]

3.2 | Rheological and injectable properties of PMH

The rheological properties of PMH were analyzed mainly by flow characteristics. Figure 2A shows the relationship between the shear rate and viscosity of HA and the different proportions of PMH. The results showed that the addition of PLLA PMs increased the viscosity of HA. With increasing shear rate, the viscosity of HA and PMH decreased, exhibiting a typical 'shear-thinning' behavior.[30] The viscosity of the PMH was the highest when the ratio of HA to PLLA was 10:5. Figure 2B shows the relationship between the shear rate and shear stress for different ratios of HA:PLLA. With an increasing shear rate, the shear stress in PMH also increased, indicating a shear thinning phenomenon. Combined with the data in Figure 2A,B, these findings verify that PMH is a non-Newtonian fluid with pseudoplastic features.[31]

We further investigated the effect of injection on the morphological changes of PLLA PMs after passing through 16G (Ø 1.65 mm), 22G (Ø 0.71 mm), or 25G (Ø 0.51 mm) needles, as well as the amount of residue in the syringe (Figures 2C–F and S2). The PLLA PMs suspended in ultrapure water could pass through a 16G needle, but it was difficult to inject them through 22G and 25G needles (Figure S2). This can be ascribed to uneven distribution of PLLA PMs in ultrapure water, resulting in accumulation during injection, which blocked the needle, finally leaving the particles squeezed at the front of the syringe. In contrast, PMH could be successfully injected using three

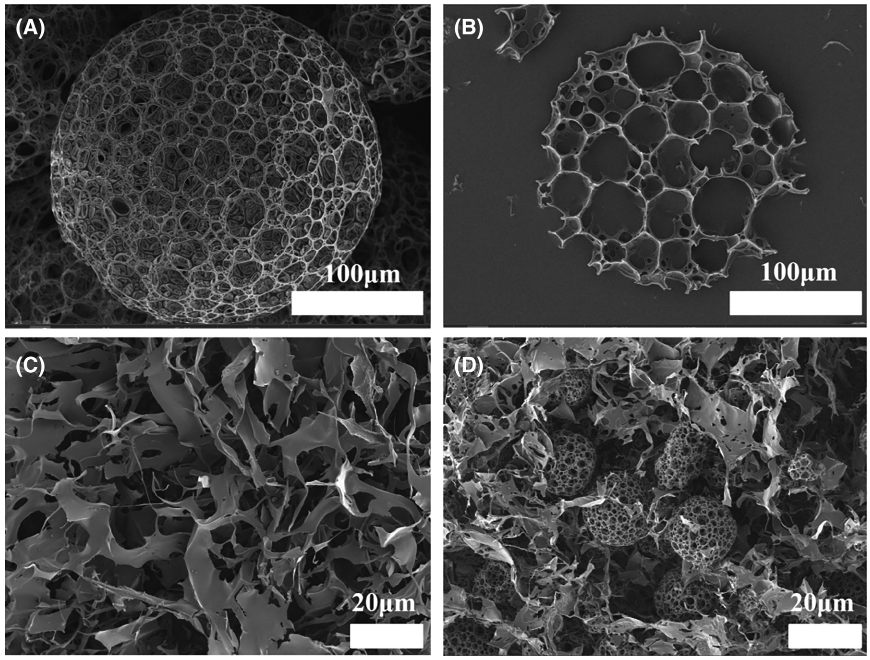

FIGURE 1 (A) SEM images of PLLA PMs. (B) the inner structure of PLLA PMs via physical section. (C, D) PMH in the absence of PLLA PMs incorporation (C), and PMH (D).

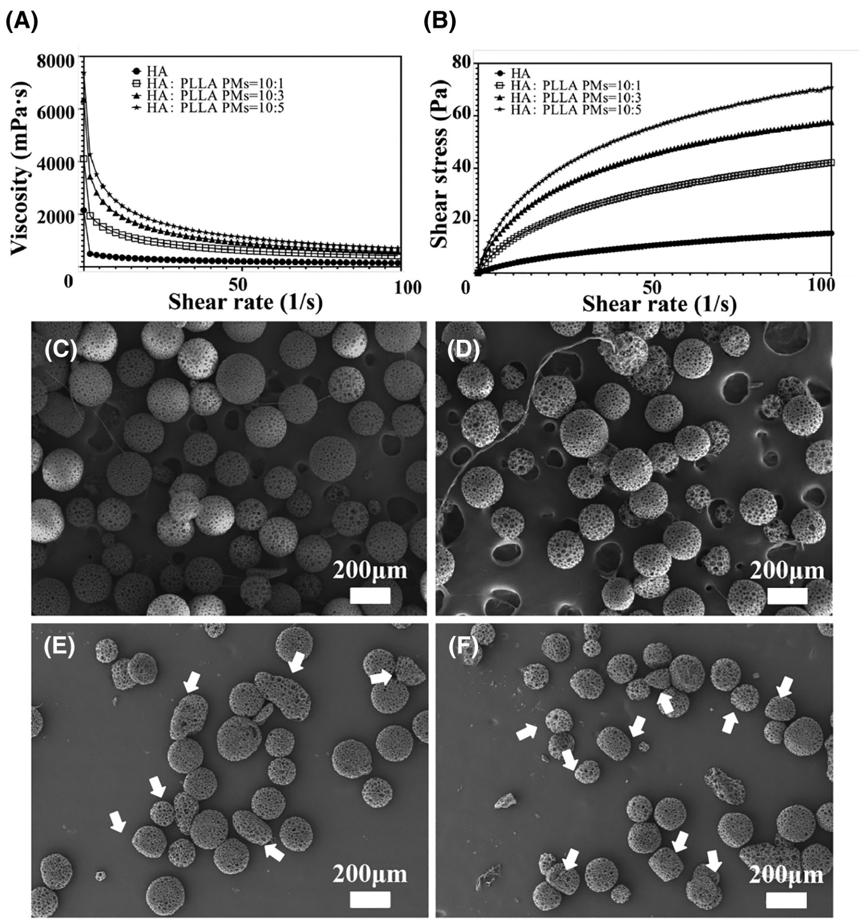

FIGURE 2 Shear rate versus viscosity (A) and shear stress (B) for HA and PMH. SEM images of PMH before injection (C) and after passing through 16G (D), 22G (E), and 25G (F) needles.

needles of different specifications. Figure 2C–F shows SEM images of the PMH group before injection and after passing through 16G, 22G, and 25G needles. We observed that the morphology of the PLLA PMs that passed through 16G needles was almost unchanged, and the PMs still exhibited a spherical shape. After passing through 22G and 25G needles, the PLLA PMs displayed irregular shapes, which may have been caused by mechanical extruding during injection.

3.3 | ADMSC proliferation and viability in PMH

The primary cultured ADMSCs exhibited a polygonal shape (Figure S3A). ADMSCs cultured to the third generation exhibited an elongated spindle-shaped morphology and a vortex-like growth pattern, indicating a better growth trend (Figure S3B). Compared with the control group, negative expression of CD34 and positive expression of CD29 (99.01%) was observed, indicating that the extracted cells were adipose mesenchymal stem cells (Figure S3C–E).[32,33] Moreover, after adipogenic induction, chondrogenic induction and osteogenic induction for 28 days, the ADMSCs exhibited superior differentiation into adipocytes, chondrocytes and osteoblasts, as confirmed by Oil Red O staining, Alcian Blue staining and Alizarin Red staining, respectively (Figure S4A–C).[34–36]

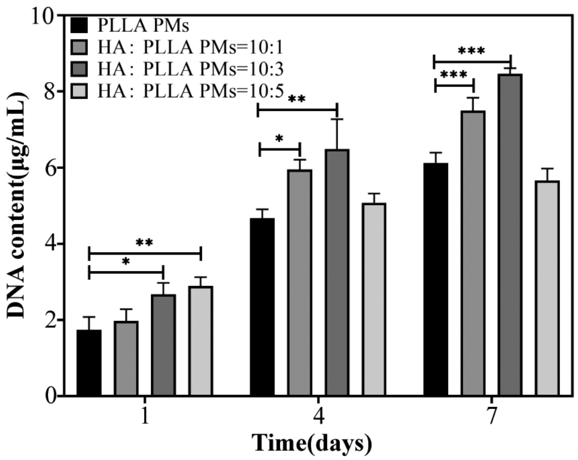

FIGURE 3 DNA content in ADMSC-incorporated PLLA PMs and ADMSC-incorporated PMH over 7 days ($n \geq 3$, *$p < 0.05$, **$p < 0.01$, ***$p < 0.001$).

Through a cell centrifugation perfusion technique for 3D microcarrier utilization described in our previous publication, ADMSCs were seeded into PLLA PMs.[15] The proliferation of ADMSCs incorporated in PLLA PMs and PMH was indirectly proven by measuring the DNA concentration in each sample. Figure 3 shows the DNA content detected after 1, 4, and 7 days of treatment with PMH containing different amounts of PLLA PMs. The results showed that the cells in the four groups exhibited good proliferation over time. Compared with the control ADMSC-incorporated PLLA PM group, the ADMSC-incorporated PMH groups exhibited significant differences in cell proliferation at different times, indicating that the composites assisted by HA were more conducive to cell adhesion and proliferation. We found that cell proliferation decreased with an increasing HA-to-PLLA ratio (10:5), indicating that there was a critical concentration for incorporation of PLLA PMs for cell growth and implantation for cartilage regeneration.

In addition, 2 days after the cells were seeded into PMH, a live/dead cell staining assay was used to confirm the viability of the ADMSCs in PMH. As shown in Figure 4, with increasing microscopic observation depth in PMs, the intensity of the green fluorescence

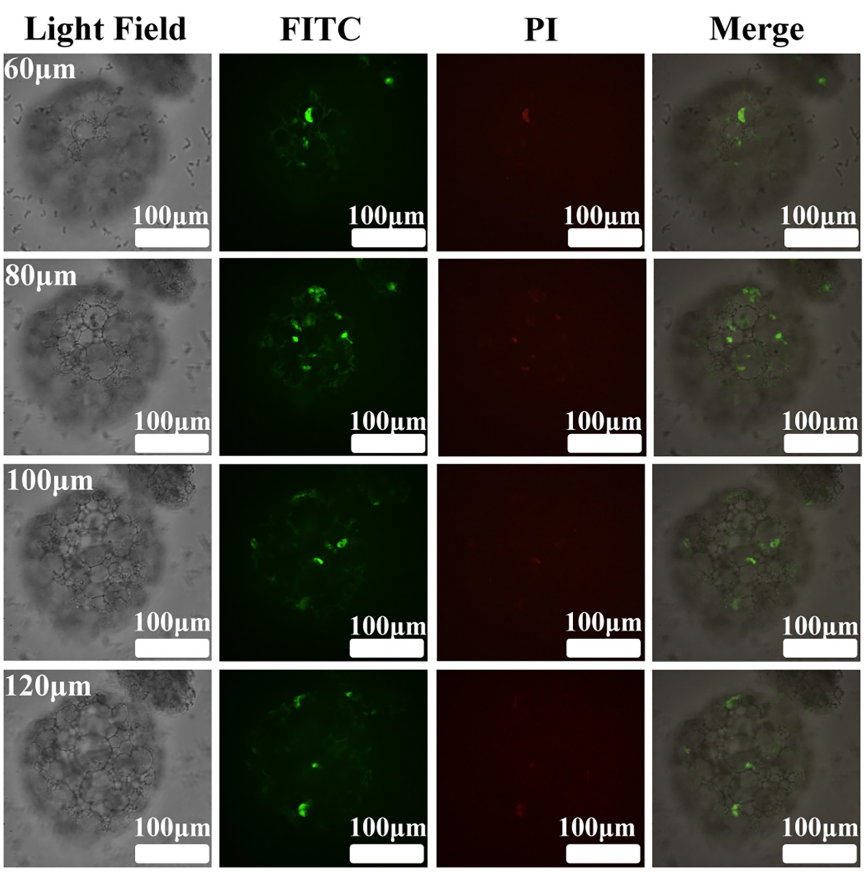

FIGURE 4 CLSM layer scanning images of ADMSC-incorporated PMH 2 days after seeding.

signal substantially increased. ADMSCs were presented at different depths and in different areas of the PLLA PMs, which indicated that the viability of the ADMSCs was good in PMH.

3.4 | Gene expression analysis and TNF-α release

To validate the chondrogenic differentiation of the ADMSCs cultured in PMH, we evaluated three different chondrogenic genes, COL2A1, ACAN, and the early cartilage formation transcription factor SOX-9, via real-time PCR. Figure 5 shows that the chondrogenic genes were upregulated in PMH over 28 days. Compared to those in the ADMSC group, the ADMSC-incorporated PMH group exhibited ca. 1.4, ca. 1.3, and ca. 2.5-fold upregulation of ACAN, COL2A, and SOX-9, respectively.

After incubation of mouse macrophages with PLLA PMs or PMH for 24 h, the levels of TNF-α released by the PLLA PM group and the control group were equivalent, while the PMH group demonstrated a significant reduction in TNF-α compared with the control group (Figure 5D) ($p < 0.01$, $n = 3$).

3.5 | *In vivo* evaluation of chondrogenesis in nude mice

Based on the gross appearance of the injection site, protuberances were observed on the skin in both groups (Figure 6A–D), indicating the formation of new tissue. The newly formed tissue in ADMSC/PMH gradually increased in size from week 4 to week 8 and was smaller than that in the ADMSC+REC/PMH group at week 4 but similar at week 8 (Figure 6E–H). The nude mice were sacrificed at 4 and 8 weeks, and the newly formed tissues were dissected for morphological viewing and histological and immunohistochemical staining. The newly formed tissues in the ADMSC/PMH group were white, transparent and soft, while those in the ADMSC+REC/PMH group were milky white, irregular and slightly hard. HE staining revealed that cells were newly generated around the PMH in both groups at 4 weeks. In both groups at 8 weeks, many new cells not only surrounded the PMH but also grew into the interior, where the cells were aggregated together and evenly distributed (Figure 6I–L). Alcian Blue staining confirmed the uniform deposition of GAG, suggesting that these cells were new chondrocytes (Figure 6M–P). Further immunohistochemical staining of type II collagen showed that the brown matrix was evenly distributed in the newly formed tissues, indicating that type II collagen matrix was formed in the newly formed tissues and that PMH induced collagen production (Figure 6Q–T).[37]

4 | DISCUSSION

In this study, we seeded ADMSCs into as-prepared PLLA PMs using our invented centrifugation perfusion technique.[6,15] HA was then mixed with ADMSC-incorporated PLLA PMs to form a hydrophilic and injectable cell delivery system (ADMSC-incorporated PMH).

For tissue regeneration, pore size is a key parameter because within the scaffold there must be enough space for cell ingrowth

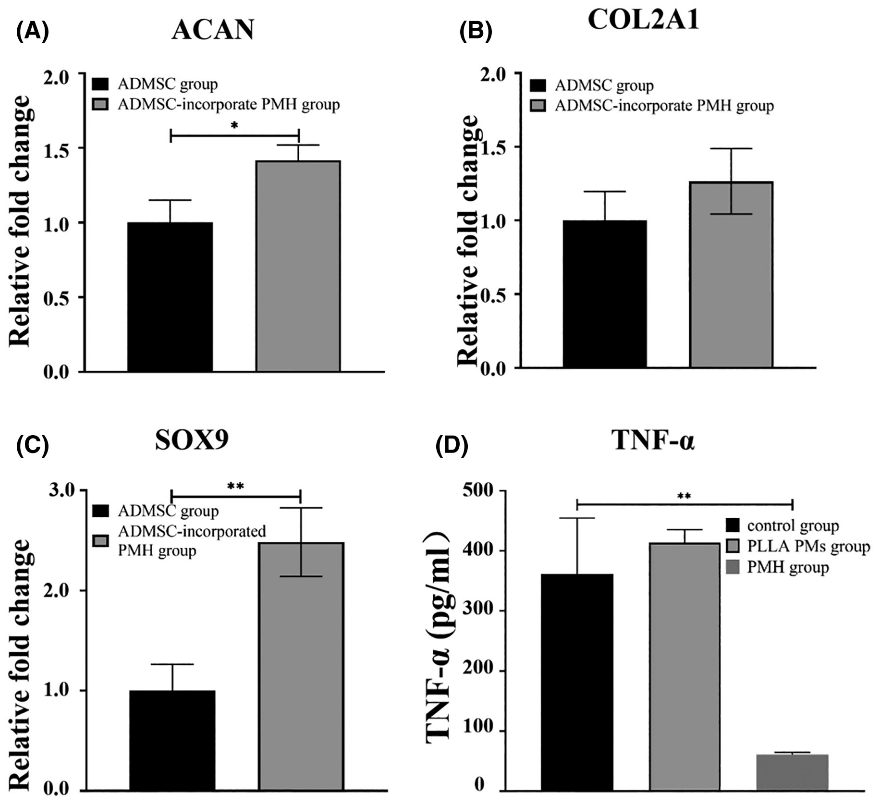

FIGURE 5 (A–C) Relative expression of chondrogenesis-related genes in seeded cells in the ADMSC group and the ADMSCs-incorporated PMH group after in vitro cultivation for 28 days, measured by real-time PCR. (D) TNF-α release from the mouse macrophage cell line RAW264.7.

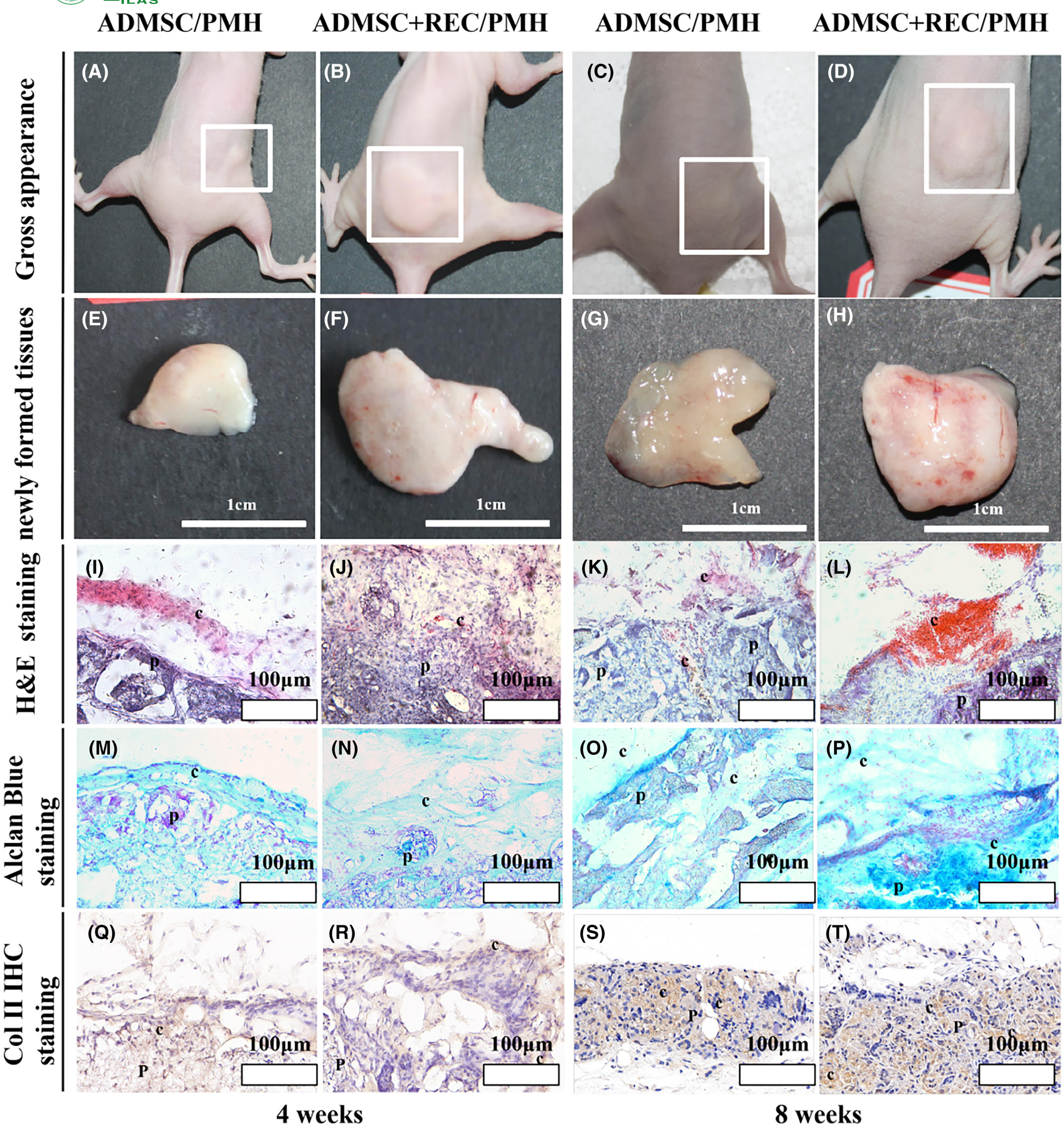

FIGURE 6 (A–D) Gross appearance of the skin of nude mice back. (E–H) Morphological view of newly formed tissues of nude mice. (I–T) Images of staining with H&E (I–L) Alclan Blue (M–P) and Col II IHC (Q–T) after cultivation in vivo for 4 and 8 weeks in the ADSC/PMH group and the ADSC+REC/PMH group; P, PMH, C, cartilage.

and proliferation, and also to facilitate oxygen or metabolite drainage.[6,9,29] The SEM images show that our prepared PLLA PMs and PMH have large pore sizes suitable for cell growth (Figures 1 and S1). In fact, we can prepare PLA or PLGA particles with the desired size, shape, surface texture and porous structure for practical applications in tissue engineering, drug delivery or for artificial cells/organs.[6,9,15,17,24,38,39] In addition, large porous microspheres provide greater adhesive space for cells, offering larger voids for cartilage regeneration.[5] The rheological stress curve reflects the rheological behavior of PMH with a change in shear rate, and conclusions can be drawn by comparing the viscoelasticity of PMH with the HA-to-PLLA ratio (Figure 2A,B).[40] Injectability experiments confirmed that PLLA PMs were uniformly suspended due to the lubricating effect of the HA, which prevented PLLA PMs clogging the needle during injection (Figures 2C–F and S2).[5] Moreover, HA is a natural extracellular matrix that is nontoxic and provides nutritional support for seeded cells.[4] As a hydrophilic biomacromolecule, HA enables cells to better adhere to hydrophobic PLLA microcarriers for further ingrowth. The 3D network structure and interconnected pores of PMH provide space for cell growth and ensure the transport of nutrients and the metabolism of waste. PMH also has typical shear-thinning properties and has the advantage of being an injectable material, making it an ideal injectable material for repairing cartilage tissue defects.[5,6,9,15,29,41]

By detecting the proliferation and viability of ADMSCs in PMH, we found that ADMSCs were present at different depths and in different areas of the PLLA PMs, and viability was good (Figures 3 and 4). PLLA PMs and PMH composites provided a suitable environment for cell adhesion and proliferation. As shown in our previous study, human periodontal ligament stem cells, and MIN6 (a mouse insulinoma cell line) and MS1 (a mouse pancreatic islet endothelial cell line) cells were successfully perfused in PMs.[6,15] We assessed the chondrogenic differentiation of ADMSCs cultured in PMH by evaluating the expression levels of chondrogenic genes, including COL2A1, ACAN, and SOX-9 (Figure 5A–C). The higher expression levels of these genes in PMH indicated that the 3D culture environment provided by PMs and the extracellular matrix provided by HA played important roles in promoting the chondrogenic differentiation of ADMSCs. Many scaffolds can induce an immune response in which TNF-α may inhibit chondrogenic differentiation of ADMSCs, leading to failure of cartilage regeneration.[42] The main orchestrators of the immune response are derived from macrophages; therefore, we cocultured the cells with the materials to determine the amount of TNF-α secreted and explore the immune compatibility of PMH.[43] The results suggested that PMH did not cause a serious immune response via TNF-α inhibition (Figure 5D). CD44 is a transmembrane glycoprotein on the cell surface, and inflammation is often accompanied by high expression of CD44 receptors on the surface of activated macrophages. HA can effectively reduce inflammation by targeted delivery through binding with CD44 receptors.[44,45] This distinct immune advantage of PMH compared with control PLLA PMs can be ascribed to the use of HA.[46] Therefore, we concluded that HA not only allowed the injection of PLLA PMs for cell delivery but also inhibited TNF-α secretion, suggesting promising chondrogenesis in vivo.[43] The results indicated that PMH can maintain cell viability and is more conducive to cell adhesion and proliferation, thereby providing a suitable environment for the differentiation of adipose stem cells into chondrocytes. This laid the foundation for our subsequent work on the generation of cartilage tissue subcutaneously in nude mice.

To evaluate the efficacy of PMH in cartilage regeneration, we subcutaneously injected ADMSC/PMH or ADMSC+REC/PMH into the backs of nude mice. The gross appearance of the injection site revealed the formation of new tissues in both the ADMSC/PMH and ADMSC+REC/PMH groups, as evidenced by protuberances on the skin. The size of the newly formed tissues in the ADMSC/PMH group increased steadily over time, while, by comparison, those in the ADMSC+REC/PMH group were larger at 4 weeks but similar at 8 weeks. Histological and immunohistochemical staining confirmed the presence of newly generated cells surrounding and growing into the PMH in both groups. The cells were aggregated together and evenly distributed within the newly formed tissues. Alcian Blue staining further confirmed the uniform deposition of GAG, indicating the presence of new chondrocytes. Immunohistochemical staining of type II collagen demonstrated the formation of a type II collagen matrix in the newly formed tissues, indicating the induction of collagen production by PMH. Despite the significant difference in the size of the newly formed tissue generated in the ADMSC/PMH group compared to that in the ADMSC+REC/PMH group, histological and immunohistochemical staining indicated that the ADMSC/PMH group did indeed generate cartilage tissue, demonstrating that the ADMSCs in PMH can differentiate into chondrocytes in vivo. Compared with ADMSC/PMH group, the larger amount of newly generated cartilage tissue in the ADMSC+REC/PMH group may be attributed to the coculture of ADMSCs with RECs, which promoted the proliferation of RECs.[47] This indicates that PMH can not only carry adipose stem cells but also support the generation of new cartilage tissue by chondrocytes subcutaneously in nude mice.

In summary, the injectable cell delivery system we developed, containing PLLA PMs loaded with ADMSCs and HA, not only possesses an appropriate three-dimensional structure and good injectability but also has the ability to promote cell proliferation, differentiation, and cartilage tissue formation both in vitro and in vivo, thus advancing the field of cartilage tissue engineering.

5 | CONCLUSIONS

PLLA PMs were prepared using a double emulsion-solvent evaporation method and ADMSCs were seeded into PLLA PMs using our invented centrifugation perfusion technique. HA was then mixed with ADMSC-incorporated PLLA PMs, which demonstrated favorable cell activity, proliferation, and chondrogenic differentiation potential in vitro. Moreover, ADMSC-incorporated PMH successfully generated subcutaneous cartilage tissue in nude mice and exhibited superior chondrogenic ability in the presence of chondrocytes. This study provides a novel approach for cartilage repair, especially for nasal cartilage regeneration, by utilizing stem cells in injectable porous fillers through the centrifugal perfusion technique.

AUTHOR CONTRIBUTIONS

All the authors listed in this paper have contributed to the preparation and execution of this research. Chang Gao: Conceptualization, writing - original draft; Wenlong Yuan, Dongcheng Wang, and Xin Zhang: Investigation; Tong Zhang contributed to the writing, review, and editing of the manuscript, as well as the acquisition of funding. Zhimin Zhou played a role in conceptualizing the study, reviewing and editing the manuscript, acquiring funding, administering the project, and providing supervision. All authors have read and agreed to the published version of the manuscript.

ACKNOWLEDGMENTS

Chang Gao greatly thanks Caijie Zhang at Tianjin Medical University, Yaoshan Liu at Peking University School and Hospital of Stomatology, JiaYue He at Chinese Academy of Medical Sciences & Peking Union Medical College for their help in this study.

FUNDING INFORMATION

This work was supported by grants from the CAMS Innovation Fund for Medical Sciences (2021-I2M-1-052), Tianjin Natural Science Foundation for Jingjinji Collaboration (23JCZXJC00240), Capital's Funds for Health Improvement and Research (CFH: 2022-2-5072), Tianjin Hospital Fund for Science and Technology (Tjyy2109) and the Open Fund of Tianjin Key Laboratory of Biomedical Materials (2022BMEKFKT002).

CONFLICT OF INTEREST STATEMENT

The authors declare no conflict of interest.

ETHICAL APPROVAL

The protocols for animal experiments were approved by the Animal Ethical and Welfare Committee of the Experimental Animal Center of the Institution of Radiation Medicine, Chinese Academy of Medical Sciences.

ORCID

Zhimin Zhou https://orcid.org/0000-0003-4832-3530

REFERENCES

1. Li H, Wang J, Song T. 3D printing technique assisted autologous costal cartilage augmentation rhinoplasty for patients with radix augmentation needs and nasal deformity after cleft lip repair. *J Clin Med*. 2022;11(24):7439. doi:10.3390/jcm11247439
2. Jessop ZM, Javed M, Otto IA, et al. Combining regenerative medicine strategies to provide durable reconstructive options: auricular cartilage tissue engineering. *Stem Cell Res Ther*. 2016;7:19. doi:10.1186/s13287-015-0273-0
3. Kontis TC. Nonsurgical Rhinoplasty. *JAMA Facial Plast Surg*. 2017;19(5):430-431. doi:10.1001/jamafacial.2017.0701
4. Cheng L, Sun X, Tang M, et al. An update review on recent skin fillers. *Plast Aesthet Res*. 2016;3:92-99. doi:10.20517/2347-9264.2015.124
5. Kang SW, La WG, Kim BS. Open macroporous poly(lactic-co-glycolic acid) microspheres as an injectable scaffold for cartilage tissue engineering. *J Biomater Sci Polym Ed*. 2009;20(3):399-409. doi:10.1163/156856209x412236
6. Liu Y, Zhang T, Li M, et al. PLGA hybrid porous microspheres as human periodontal ligament stem cell delivery carriers for periodontal regeneration. *Chem Eng J*. 2021;420:129703. doi:10.1016/j.cej.2021.129703
7. Martin Y, Eldardiri M, Lawrence-Watt DJ, Sharpe JR. Microcarriers and their potential in tissue regeneration. *Tissue Eng Part B Rev*. 2011;17(1):71-80. doi:10.1089/ten.TEB.2010.0559
8. Zhou Z, Wu W, Fang J, Yin J. Polymer-based porous microcarriers as cell delivery systems for applications in bone and cartilage tissue engineering. *Int Mater Rev*. 2021;66(2):77-113. doi:10.1080/09506608.2020.1724705
9. Yao X, Yang Y, Zhou Z. Non-mulberry silk fiber-based composite scaffolds containing Millichannels for auricular cartilage regeneration. *ACS Omega*. 2022;7(17):15064-15073. doi:10.1021/acsomega.2c00846
10. O'Brien FJ. Biomaterials & scaffolds for tissue engineering. *Mater Today*. 2011;14(3):88-95. doi:10.1016/S1369-7021(11)70058-X
11. Zhao H, Ma L, Gao C, Shen J. A composite scaffold of PLGA microspheres/fibrin gel for cartilage tissue engineering: fabrication, physical properties, and cell responsiveness. *J Biomed Mater Res B Appl Biomater*. 2009;88(1):240-249. doi:10.1002/jbm.b.31174
12. Leong W, Lau TT, Wang DA. A temperature-cured dissolvable gelatin microsphere-based cell carrier for chondrocyte delivery in a hydrogel scaffolding system. *Acta Biomater*. 2013;9(5):6459-6467. doi:10.1016/j.actbio.2012.10.047
13. McLaren JS, Macri-Pellizzeri L, Hossain KMZ, et al. Porous phosphate-based glass microspheres show biocompatibility, tissue infiltration, and osteogenic onset in an ovine bone defect model. *ACS Appl Mater Interfaces*. 2019;11(17):15436-15446. doi:10.1021/acsami.9b04603
14. Chung HJ, Park TG. Injectable cellular aggregates prepared from biodegradable porous microspheres for adipose tissue engineering. *Tissue Eng Part A*. 2009;15(6):1391-1400. doi:10.1089/ten.tea.2008.0344
15. Guo C, Zhang T, Tang J, Gao C, Zhou Z, Li C. Construction of PLGA porous microsphere-based artificial pancreatic islets assisted by the cell centrifugation perfusion technique. *ACS Omega*. 2023;8(17):15288-15297. doi:10.1021/acsomega.3c00424
16. Chung HJ, Kim IK, Kim TG, Park TG. Highly open porous biodegradable microcarriers: *in vitro* cultivation of chondrocytes for injectable delivery. *Tissue Eng Part A*. 2008;14(5):607-615. doi:10.1089/tea.2007.0263
17. Zeng Y, Li X, Liu X, et al. PLLA porous microsphere-reinforced silk-based scaffolds for auricular cartilage regeneration. *ACS Omega*. 2021;6(4):3372-3383. doi:10.1021/acsomega.0c05890
18. Gupta V, Khan Y, Berkland CJ, Laurencin CT, Detamore MS. Microsphere-based scaffolds in regenerative engineering. *Annu Rev Biomed Eng*. 2017;19:135-161. doi:10.1146/annurev-bioeng-071516-044712
19. Yang TH, Miyoshi H, Ohshima N. Novel cell immobilization method utilizing centrifugal force to achieve high-density hepatocyte culture in porous scaffold. *J Biomed Mater Res*. 2001;55(3):379-386. doi:10.1002/1097-4636(20010605)55:3<379::aid-jbm1026>3.0.co;2-z
20. Capuana E, Lopresti F, Ceraulo M, la Carrubba V. Poly-l-lactic acid (PLLA)-based biomaterials for regenerative medicine: a review on processing and applications. *Polymers (Basel)*. 2022;14(6):1153. doi:10.3390/polym14061153
21. Ju HW, Sheikh FA, Moon BM, et al. Fabrication of poly(lactic-co-glycolic acid) scaffolds containing silk fibroin scaffolds for tissue engineering applications. *J Biomed Mater Res A*. 2014;102(8):2713-2724. doi:10.1002/jbm.a.34947
22. Yan S, Wang L, Fan H, et al. Biomimetic natural silk nanofibrous microspheres for multifunctional biomedical applications. *ACS Nano*. 2022;16(9):15115-15123. doi:10.1021/acsnano.2c06331
23. Zhang S, Lin A, Tao Z, et al. Microsphere-containing hydrogel scaffolds for tissue engineering. *Chem Asian J*. 2022;17(20):e202200630. doi:10.1002/asia.202200630
24. Yang Y, Yao X, Li X, et al. Non-mulberry silk fiber-based scaffolds reinforced by PLLA porous microspheres for auricular cartilage: an *in vitro* study. *Int J Biol Macromol*. 2021;182:1704-1712. doi:10.1016/j.ijbiomac.2021.05.145
25. Kokai LE, Marra K, Rubin JP. Adipose stem cells: biology and clinical applications for tissue repair and regeneration. *Transl Res*. 2014;163(4):399-408. doi:10.1016/j.trsl.2013.11.009
26. Guneta V, Tan NS, Chan SK, et al. Comparative study of adipose-derived stem cells and bone marrow-derived stem cells in similar microenvironmental conditions. *Exp Cell Res*. 2016;348(2):155-164. doi:10.1016/j.yexcr.2016.09.012
27. Dias IX, Cordeiro A, Guimarães JAM, Silva KR. Potential and limitations of induced pluripotent stem cells-derived mesenchymal

stem cells in musculoskeletal disorders treatment. *Biomolecules*. 2023;13(9):1342. doi:10.3390/biom13091342
28. Drela K, Stanaszek L, Nowakowski A, Kuczynska Z, Lukomska B. Experimental strategies of mesenchymal stem cell propagation: adverse events and potential risk of functional changes. *Stem Cells Int*. 2019;2019:7012692. doi:10.1155/2019/7012692
29. Choi S-W, Zhang Y, Yeh Y-C, Lake Wooten A, Xia Y. Biodegradable porous beads and their potential applications in regenerative medicine. *J Mater Chem*. 2012;22(23):11442-11451. doi:10.1039/C2JM16019F
30. Dodero A, Williams R, Gagliardi S, Vicini S, Alloisio M, Castellano M. A micro-rheological and rheological study of biopolymers solutions: hyaluronic acid. *Carbohydr Polym*. 2019;203:349-355. doi:10.1016/j.carbpol.2018.09.072
31. Su X, Chen W, Xu W. Characterizing the rheological behaviors of non-Newtonian fluid via a viscoelastic component: fractal dashpot. *Adv Mech Eng*. 2017;9(10):1687814017699765. doi:10.1177/1687814017699765
32. Burja B, Barlič A, Erman A, et al. Human mesenchymal stromal cells from different tissues exhibit unique responses to different inflammatory stimuli. *Curr Res Transl Med*. 2020;68(4):217-224. doi:10.1016/j.retram.2020.05.006
33. Zhang Q, Hubenak J, Iyyanki T, et al. Engineering vascularized soft tissue flaps in an animal model using human adipose-derived stem cells and VEGF+PLGA/PEG microspheres on a collagen-chitosan scaffold with a flow-through vascular pedicle. *Biomaterials*. 2015;73:198-213. doi:10.1016/j.biomaterials.2015.09.024
34. Choi YS, Park SN, Suh H. Adipose tissue engineering using mesenchymal stem cells attached to injectable PLGA spheres. *Biomaterials*. 2005;26(29):5855-5863. doi:10.1016/j.biomaterials.2005.02.022
35. Zhou X, Wang J, Huang X, et al. Injectable decellularized nucleus pulposus-based cell delivery system for differentiation of adipose-derived stem cells and nucleus pulposus regeneration. *Acta Biomater*. 2018;81:115-128. doi:10.1016/j.actbio.2018.09.044
36. Zannettino AC, Paton S, Arthur A, et al. Multipotential human adipose-derived stromal stem cells exhibit a perivascular phenotype *in vitro* and *in vivo*. *J Cell Physiol*. 2008;214(2):413-421. doi:10.1002/jcp.21210
37. Zhang Y, Liang H, Luo Q, et al. *In vivo* inducing collagen regeneration of biodegradable polymer microspheres. *Regen Biomater*. 2021;8(5):rbab042. doi:10.1093/rb/rbab042
38. Zhang J, Wang J, Qiao F, et al. Polymeric non-spherical coarse microparticles fabricated by double emulsion-solvent evaporation for simvastatin delivery. *Colloids Surf B Biointerf*. 2021;199:111560. doi:10.1016/j.colsurfb.2021.111560
39. Zhang T, Li M, Wang X, Zhou Z, Yuan W, Ma J. Facile synthesis of polylactide coarse microspheres as artificial antigen-presenting cells. *Chem Commun (Camb)*. 2018;54(80):11356-11359. doi:10.1039/c8cc04958k
40. Ciccone G, Dobre O, Gibson GM, et al. What caging force cells feel in 3D hydrogels: a rheological perspective. *Adv Healthc Mater*. 2020;9(17):e2000517. doi:10.1002/adhm.202000517
41. Chen MH, Wang LL, Chung JJ, Kim YH, Atluri P, Burdick JA. Methods to assess shear-thinning hydrogels for application as injectable biomaterials. *ACS Biomater Sci Eng*. 2017;3(12):3146-3160. doi:10.1021/acsbiomaterials.7b00734
42. Guo J, Ye W, Wu X, et al. TNF-α activates RELA expression via TNFRSF1B to upregulate OPA1 expression and inhibit chondrogenic differentiation of human adipose stem cells. *J Orthop Surg Res*. 2023;18(1):430. doi:10.1186/s13018-023-03846-x
43. Chisari E, Yaghmour KM, Khan WS. The effects of TNF-alpha inhibition on cartilage: a systematic review of preclinical studies. *Osteoarthr Cartil*. 2020;28(5):708-718. doi:10.1016/j.joca.2019.09.008
44. Wolf KJ, Kumar S. Hyaluronic acid: incorporating the bio into the material. *ACS Biomater Sci Eng*. 2019;5(8):3753-3765. doi:10.1021/acsbiomaterials.8b01268
45. Marinho A, Nunes C, Reis S. Hyaluronic acid: a key ingredient in the therapy of inflammation. *Biomolecules*. 2021;11(10):1518. doi:10.3390/biom11101518
46. Rayahin JE, Buhrman JS, Zhang Y, Koh TJ, Gemeinhart RA. High and low molecular weight hyaluronic acid differentially influence macrophage activation. *ACS Biomater Sci Eng*. 2015;1(7):481-493. doi:10.1021/acsbiomaterials.5b00181
47. Shi J, Liang J, Guo B, et al. Adipose-derived stem cells cocultured with chondrocytes promote the proliferation of chondrocytes. *Stem Cells Int*. 2017;2017:1709582. doi:10.1155/2017/1709582

SUPPORTING INFORMATION

Additional supporting information can be found online in the Supporting Information section at the end of this article.

How to cite this article: Gao C, Yuan W, Wang D, Zhang X, Zhang T, Zhou Z. Adipose-derived mesenchymal stem cell-incorporated PLLA porous microspheres for cartilage regeneration. *Anim Models Exp Med*. 2024;7:685-695. doi:10.1002/ame2.12433